AIAA Aviation
22-26 June 2015, Dallas, TX
21st AIAA/CEAS Aeroacoustics Conference

# An Approach to Estimate the Reliability of Microphone Array Methods

Gert Herold* and Ennes Sarradj†
*Brandenburg University of Technology, D-03046 Cottbus, Germany*

**Establishing microphone array methods as tool for precise acoustic measurements necessitates assessing their reliability depending on given boundary conditions. In this contribution, an approach to evaluate the performance of microphone array methods is proposed. Instead of simply testing an algorithm on distinct scenarios, Monte Carlo simulations are performed to allow for a statistical analysis. In a simulation scenario, number of sources, source positions, and source levels are varied. The objective is set to correctly reconstruct the level and position of the sound sources, and a rating criterion is defined. The microphone array methods DAMAS, CLEAN-SC, Orthogonal Beamforming and Covariance Matrix Fitting are tested for their performance on 12 600 generated data sets. The results are then statistically evaluated regarding the precision of the reconstruction abilities depending on the varied parameters. It is shown that this approach helps deducing information about the characteristic performance of the methods that could not easily have been revealed otherwise.**



## Nomenclature

| | | | |
|---|---|---|---|
| $\boldsymbol{A}$ | transfer matrix | $N$ | number of focus grid points |
| $\boldsymbol{b}$ | beamformer output | $\boldsymbol{p}$ | complex sound pressures |
| $c$ | speed of sound | $\boldsymbol{P}$ | matrix of point spread functions |
| $\boldsymbol{C}_{\mathrm{vec}}$ | vectorized cross spectral matrix | $w$ | beamwidth |
| $d$ | Array aperture | $\boldsymbol{x}_t$ | focus point (3D vector) |
| $f$ | frequency | $\alpha$ | regularization parameter |
| $\boldsymbol{h}$ | steering vector | $\sigma$ | standard deviation |
| $He$ | Helmholtz number | $\sigma_{\mathrm{R}}$ | mode of Rayleigh distribution |
| $L_p$ | sound pressure level | | |
| $\Delta L_{p,\mathrm{err}}$ | level error from reconstruction | CSM | cross spectral matrix |
| $M$ | number of microphones | PDF | probability density function |

## I. Introduction

The application of microphone array based tools for the characterization of sound sources has become state of the art in aeroacoustic measurements. The objective is to detect the exact position of the sources as well as the level of the radiated sound by synchronously measuring sound pressures at spatially distributed positions.

The most commonly used methods based on microphone array measurements are beamforming algorithms, which shift the microphone signals such that they "focus" on a chosen point in space, taking into account the retarded time from the focus point to the microphones. Since the output of a simple delay-and-sum beamformer can be interpreted as a convolution of the real source distribution with a point spread function, depending on focus point and array characteristics, it is common to "deconvolve" the result using

*PhD Student, Chair of Technical Acoustics, Brandenburg University of Technology.
†Professor, Chair of Technical Acoustics, Brandenburg University of Technology.

more sophisticated algorithms to obtain the actual source positions and levels. Such deconvolution methods include DAMAS,[1] CLEAN-SC,[2] and Orthogonal Beamforming.[3] A different approach is pursued with inverse methods, such as Covariance Matrix Fitting,[4] which solve an optimization problem by fitting an unknown source distribution to the measured data using an assumed sound propagation model.

Theoretically, all these methods should yield the same result when used for the same case. However, as was shown in earlier works,[5–7] different array-based algorithms yield different results when applied to identical input data. Seeking to advance microphone array methods for their use as precise measuring tool, it is imperative to determine the reliability of existing and future methods. The idea of this contribution is to deliver an exemplary "reliability study" for one distinct microphone array geometry, i.e., to quantify the theoretical ability of the array to determine the correct location and level of acoustic sources given a set of input parameters.

The following section contains a description of the framework for setting up a reliability study for microphone array methods. Moreover, a reference setup representing a standard use case is outlined. The compared microphone array methods and their working principles are described, as well as the used setup for the simulations and the statistical method for evaluation. Section III comprises an evaluation of the performance of four chosen array methods depending on several parameters, using an exemplary rating criterion. The findings are summarized in the concluding section.



## II. Methodology

For a methodical evaluation of the performance of the microphone array methods it is necessary to identify the parameters on which the results may depend and to define the boundary conditions under which the derived conclusions are valid. The steps taken to build such an evaluation system are itemized in this section.

### A. Environment setup

The most fundamental parameters that have to be decided on are those describing the microphone array, since in general they cannot be changed easily. These include the number of microphones, the rules of distributing them in space, and the aperture. The latter, together with the speed of sound, is directly coupled with the performance at chosen frequencies and the possible spatial resolution.

For the purpose of this study, the microphone geometry was chosen to be invariable. As is illustrated in figure 1, it features 64 microphones, with one microphone at the array center and the rest distributed over seven logarithmic spiral arms. All distances in this paper are given in units of the array aperture $d$. Frequencies are described in the non-dimensional form of Helmholtz numbers

$$He = \frac{f\,d}{c}\ ,$$

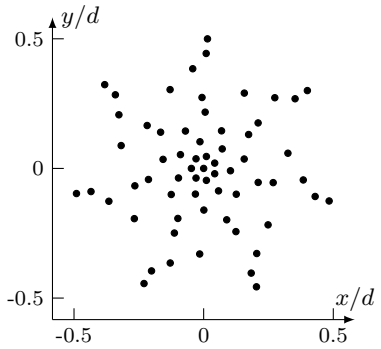


**Figure 1. Array geometry with 64 microphones in one plane, aperture *d*.**

normalized with the array aperture $d$ and the speed of sound $c$.

Next, the area to focus on has to be chosen, i.e., the number of focus points and their distribution in space. These usually vary depending on the expected source area. Only sources in a plane parallel to the microphone array are considered here. The focus area consists of a regularly-spaced square grid with a side length of one aperture $d$ and a distance to the array of $0.5\,d$. The distance of the grid points was fixed at $\Delta x = \Delta y = 0.02\,d$, which results in a focus grid of 2601 points.

For practical measurements it is sometimes necessary to account for a flow field or other properties influencing the sound propagation. However, this would be beyond the scope of this study and is not included here. The fluid is considered to be homogeneous with a linear propagation of sound. The parameters describing the basic environment setup are summarized in table 1.

## B. Data generation

Among other things, the performance of a microphone array method depends on the actual source distribution. All methods used here assume a simple monopole source model with uncorrelated sources, which does not necessarily correspond with actual properties of a real sound field they may be applied on. However, results are not the same for different methods, even when using simulated sources that fulfill these restrictions. The scenarios used in this study take into account multiple point sources emitting uncorrelated white noise signals.

The scenario properties varied in this study are:

- number of sources
- source positions
- relative source levels

Even with the restriction to the variation of three properties, the parameter space is extensive and cannot be covered completely. In order to obtain meaningful results concerning the performance reliability of the algorithms, a statistical approach is necessary. Therefore, the data were generated applying a Monte-Carlo method, drawing the varied parameters from different random distributions.

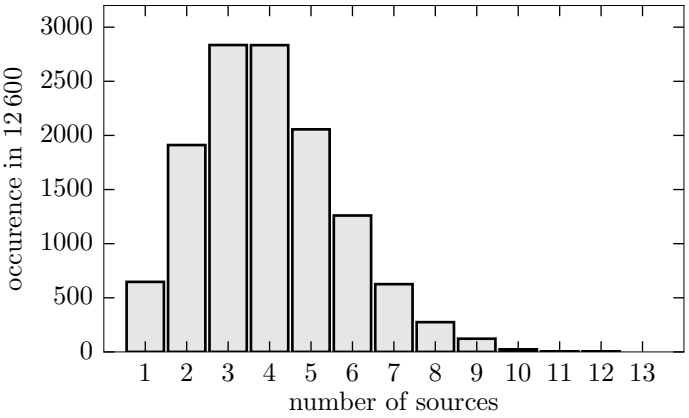


**Figure 2. Histogram for number of sources drawn from the Poisson distribution ($\lambda = 3$, 12 600 samples).**

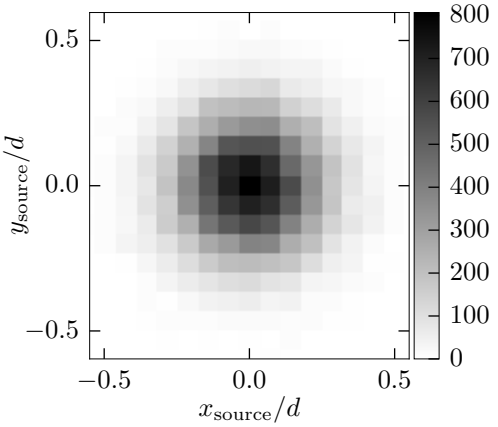


**Figure 3. 2D-histogram for 30 000 source positions drawn from the bivariate normal distribution ($\sigma = 0.1688$, values constrained to $x, y \in [-0.5\,d, 0.5\,d]$.)**

The number of sources for each data set is drawn from a Poisson distribution, which yields discrete integer values (including 0, thus a value of 1 is added to the drawn number). The parameter $\lambda = 3$ is chosen for 3 and 4 to be the most probable number of sources (see figure 2).

The sources are all distributed in the focus plane, i.e. $z = d/2$. For each source, $(x, y)$ is drawn from a bivariate normal distribution (see figure 3). The standard deviation $\sigma = 0.1688$ is chosen such that 2/3 of the positions lie inside the circle with a diameter of $d/2$. This is based on the assumption that array measurements usually are designed in a way that possible sources are positioned inside the focus area and as central as possible. The position of the sources do not necessarily coincide with a focus grid position.

For the different source levels, Rayleigh-distributed values are drawn (the probability density function for the used mode $\sigma_{\mathrm{R}} = 5$ is shown in figure 4) for each data set. These are interpreted as squared sound pressures in a fixed distance from the respective source. For the exemplary case of four sources, figure 5 shows the histograms of the minimum and maximum level differences occurring between sources.

In more than 50 % of the cases the levels of at least two sources differ 1 dB or less; higher level differences become rapidly less probable. The highest level difference between any source is between 5 dB and 15 dB in most of the cases. Differences of more than 20 dB are rather improbable. These characteristics of the chosen random distribution are in good agreement with the premise that in general there are several sources with comparable levels and sources more than 20 dB below any other source are not of interest.

The simulated noise signals at the microphone positions are sampled at a frequency corresponding to $He = 40$. For further processing, the signal is divided into blocks of 1024 samples which overlap by 50 %.

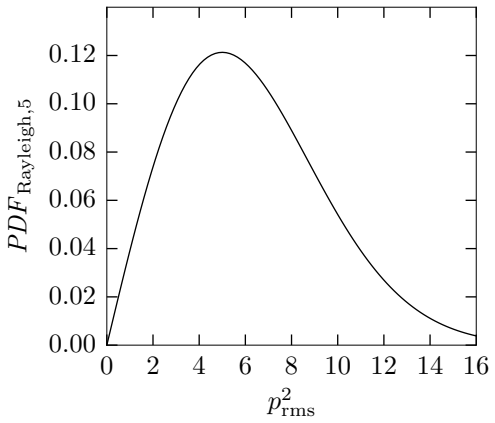


**Figure 4. Probability density function for the Rayleigh distribution (mode $\sigma_{\mathrm{R}} = 5$).**

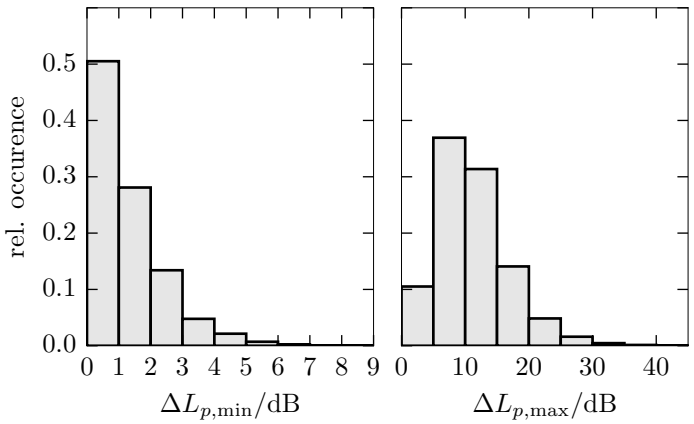


**Figure 5. Scaled histogram of the minimum (left) and the maximum (right) level differences occuring between 4 source levels randomly drawn from the Rayleigh distribution.**



With each time signal consisting of 512 000 samples this results in 1000 blocks. Prior to an FFT, von-Hann windowing is applied to the blocks to diminish spectral leakage caused by the transformation. The sampling rate and block size are chosen such that the third-octave band around the lowest considered Helmholtz number $He = 1$ still contains six discrete values.

Important data generation parameters and their attributed values for this study are listed in table 2.

### C. Microphone array methods

All algorithms compared in this contribution work in the frequency domain, evaluating the cross-spectral matrix (CSM). This matrix is approximated by averaging the cross spectra

$$\boldsymbol{C} = \overline{\boldsymbol{p}\boldsymbol{p}^{\mathrm{H}}} \ ,$$

with the vector $\boldsymbol{p}$ containing the complex sound pressures at the microphone positions. The superscript $^{\mathrm{H}}$ denotes the Hermitian transpose.

The classic delay-and-sum beamformer formulation in the frequency domain is

$$b(\boldsymbol{x}_t) = \boldsymbol{h}^{\mathrm{H}}(\boldsymbol{x}_t)\, \boldsymbol{C}\, \boldsymbol{h}(\boldsymbol{x}_t) \ , \qquad t = 1 \ldots N \ . \tag{1}$$

$N$ denotes the number of arbitrary focus points $\boldsymbol{x}_t$, at which this equation is to be evaluated. Usually they describe a regularly spaced grid containing a region with possible sound source locations.

The steering vector $\boldsymbol{h}$ can be derived from measured transfer functions or it can be calculated based on theoretical models. As there exist several formulations to calculate steering vectors, the choice of $\boldsymbol{h}$ already constitutes a possible parameter influencing the performance of the chosen method. A compilation of several steering vectors analyzing their respective characteristics was done by Sarradj.[8] Only one steering vector was considered for the following calculations, corresponding to formulation III in the above-mentioned study. Its entries are calculated via

$$h_m = \frac{1}{r_{t,0} r_{t,m} \sum_{l=1}^{M} {r_{t,l}}^{-2}}\, \mathrm{e}^{-\mathrm{j}k(r_{t,m} - r_{t,0})} \ , \qquad m = 1 \ldots M \ , \tag{2}$$

with the number of microphones $M$ and $r_{t,m}$ describing the distance between the focus points and the microphones (or, for $r_{t,0}$, the array center).

Since the main diagonal of the CSM containing the autospectra of the microphones does not add any information about the phase differences and the amplitudes of the sources it can be left out for the calculations. This has the advantage that uncorrelated noise from measurements is also be reduced.

The output map of equation (1) features artifacts (i.e. side lobes) depending on the microphone geometry and the chosen focus points and can be interpreted as the correct source level distribution being convoluted with a point spread function intrinsic to the microphone array and the focus grid.

**DAMAS** The DAMAS algorithm was introduced by Brooks and Humphreys.[1] Writing the output of (1) into a vector $\boldsymbol{b}$ with $N$ entries, the convolution of the correct level distribution can be described as a system of equations:

$$\boldsymbol{b} = \boldsymbol{P}\boldsymbol{b'} \ , \tag{3}$$

where the columns of the matrix $\boldsymbol{P}$ contain the known point spread functions from each focus point to all other focus points. The vector $\boldsymbol{b'}$ contains the unknown deconvoluted result, which is determined by iteratively solving equation (3) with a modified Gauss-Seidel algorithm. The number of iterations has to be chosen and is set to 500 for all calculations.

**CLEAN-SC** This method was developed by Sijtsma[2] and makes use of the coherence of the side lobes induced by the actual sources. It is also an iterative algorithm. Each iteration consists of looking for the maximum in the convoluted map, storing it in a new map, and subtracting it and its coherent parts from the original map. Performance of this method is governed by a damping factor between 0 and 1, which allows for the subtraction of only a fraction of the found value and coherent portions in each iteration step to account for superposed sources, and the number of iterations. For the calculations in this paper, the damping factor is set to 0.6 and the number of iterations to 500.

**OB** The Orthogonal Beamforming technique does not require prior beamforming and was introduced by Sarradj.[3] It is based on the assumption that each of a number of eigenvalue of the CSM can be attributed to a source which is uncorrelated to the others. The eigenvalues and eigenvectors from the decomposition of the CSM are used for determining the source level and its location through component-wise beamforming. The number of sources being considered is controlled by the number of eigenvalues used for processing, which is set to 20 for the evaluations performed here.

**CMF** The Covariance Matrix Fitting method and variants were described in several publications.[4,6,9] It is an inverse algorithm and works independent from beamforming techniques. The idea is to solve the convex optimization problem

$$\min_{\boldsymbol{b'}} \|\boldsymbol{C}_{\mathrm{vec}} - \boldsymbol{A}\boldsymbol{b'}\|_2^2 + \alpha \|\boldsymbol{b'}\|_1 \ , \qquad \alpha > 0 \ , \tag{4}$$

where $\boldsymbol{C}_{\mathrm{vec}}$ is the vectorized CSM and $\boldsymbol{A}$ the transfer matrix from the focus grid positions to the microphones. The regularization parameter $\alpha$ is used to enforce sparsity of the solution while searching for the best possible fit for the data. For this contribution, the system described by equation (4) is solved using a Least Angle Regression Lasso algorithm (LARS-Lasso[10]), and $\alpha$ is determined applying the Bayesian information criterion.[11] The maximum number of iterations is set to be 500.

The microphone array method parameters are summarized in table 3.

### D. Evaluation

The basis for the evaluation of the methods are the calculated maps showing the reconstructed sources on the focus grid for third-octave bands. Considered were the bands with central Helmholtz numbers between 1 and 16.

The main objective of any microphone array method is to determine both the position and the level of the sources correctly. One possibility to assess the two quantities is to compare the expected theoretic sound pressure level at a source position with the level reconstructed by a chosen algorithm:

$$\Delta L_{p,\mathrm{err}} = L_{p,\mathrm{reconstructed}} - L_{p,\mathrm{theoretic}} \ . \tag{5}$$

This has the advantage that information about an over- or underestimation of the actual sound pressure level of a source is stored in a single parameter. It has to be kept in mind, however, that this kind of evaluation gives no explicit information about the overall quality of the reconstructed map concerning artifacts or noisiness. Furthermore, the value calculated in equation (5) is influenced by the fashion in which $L_{p,\mathrm{reconstructed}}$ is determined. Since the source position is not necessarily contained in the set of focus grid points, an appropriate sub-set of grid points surrounding the source position has to be chosen. The calculated squared sound pressures at those positions are then summed to represent the reconstructed sound pressure.
The criterion applied here is based on the delay-and-sum beamforming result caused by a monopole source at the grid center in the third-octave band around $He = 8$, applying all boundary conditions as mentioned above. The beamwidth $w$ is determined by measuring the distance between the two opposite positions at

**Table 1. Environment parameters.**

| | |
|---|---|
| Environment | resting, homogeneous fluid |
| Array | 7 logarithmic spirals, see fig. 1, 64 microphones |
| Focus grid | regularly spaced square $x, y \in [-0.5d, 0.5d], z = 0.5d$ $\Delta x = \Delta y = 0.02\,d$ |

**Table 2. Data generation parameters.**

| | |
|---|---|
| Source type | monopole |
| Signals | uncorrelated white noise |
| No. of sources | **varied** (see fig 2) |
| Source positions | $z = d/2$; $x, y$ **varied** (fig. 3) |
| Source levels | **varied** (see figures 4 & 5) |
| Sampling rate | $He_{\text{sample}} = 40$ |
| No. of samples | 512 000 |
| Block size | 1024 samples |
| Block overlap | 50 % |
| Windowing | von Hann / Hanning |

**Table 3. Microphone array method parameters.**

| | |
|---|---|
| Type of methods | CSM-based |
| CSM main diagonal | removed |
| Steering vector | eq. (2) |
| DAMAS iterations | 500 |
| CLEAN-SC iterations | 500 |
| CLEAN-SC damping | 0.6 |
| OB no. of eigenvalues | 20 |
| CMF max. iterations | 500 |
| CMF regularization | BIC[11] |

**Table 4. Evaluation parameters.**

| | |
|---|---|
| Evaluation basis | sound maps for third-octave bands |
| Frequencies | $He_{\min} = 1$, $He_{\max} = 16$ |
| Evaluation type | integration of subdomains at expected source positions |
| Integration sectors | circles with $\oslash = 0.1d$ |

which the sound pressure level drops to 3 dB below the maximum, as is shown in figure 6. The value of $w = 0.1d$ is now used as reference for defining the diameter of a circle around the supposed source location, which also encloses all grid positions of the reconstructed sound pressure values to be summed. Figure 7 shows an exemplary map calculated with the CLEAN-SC algorithm for the third-octave band around $He = 2$. The circles mark the integration areas around the four source positions, which were randomly drawn prior to the simulations. The respective integrated sound pressure levels are indicated below the circles, with the expected levels in parentheses. The level errors $\Delta L_{p,\text{err}}$ from top to bottom source therefore are: 0 dB, −6 dB, −12 dB, −17 dB.

Table 4 contains a list of the used evaluation parameters.

### E. Computational setup

Calculations were performed on a computer cluster with 104 2.2 GHz CPUs. A total of 12 600 data sets were generated, following the procedure described in section B. Each of the data sets was evaluated with four different methods (see section C). The overall computation time spent on the evaluations was 62 700 CPU hours, with DAMAS being the most time-consuming algorithm (69 % of overall computing time), followed by CMF (29 %). The run times of the CLEAN-SC (1.5 %) and OB (0.5 %) are negligible in comparison.

All simulations and evaluations were performed using the Acoular[12] software package, which is being developed at the Chair of Technical Acoustics at Brandenburg University of Technology.

## III. Results

The figures in this section show a statistical evaluation of the sound pressure level errors calculated according to the procedure described in section II.D. The median of the level errors is plotted against various characteristic parameters. Additionally, the range between the 16th and 84th percentiles is depicted filled to indicate the interval in which 68 % of the respective level errors are contained. For a normal distribution this would correspond to the values within one standard deviation to each side of the mean value. In case of the investigated parameters being continuously distributed (e.g. the distance from one source to the closest other source), the associated level errors are collected in appropriate interval bins to allow for a statistical analysis. For clarity, the curves associated with the respective array methods are drawn on method-specific axes, indicated by accordingly colored scales.

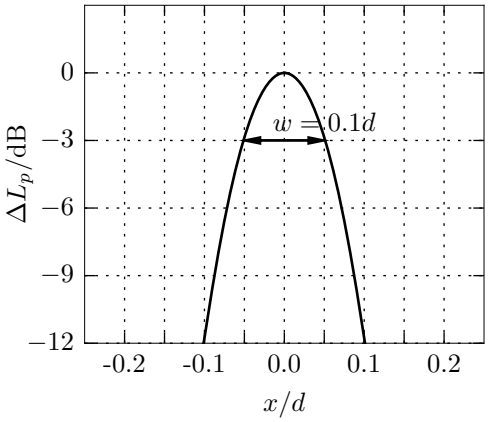


**Figure 6. Main lobe and beamwidth for the third-octave band around $He = 8$.**

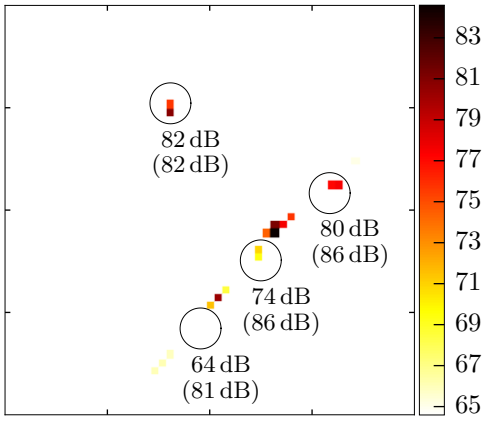


**Figure 7. Example of a CLEAN-SC Map for $He = 2$, 1/3 octave. Circles indicate integration areas around the correct source positions.**



Figure 8 shows the dependence of the level error on the Helmholtz number for the strongest source, the second strongest, and the weakest source of the respective data sets. As can be expected, the absolute error increases with lower $He$ for all methods. In comparison, CMF performs best, judging from the error median being very close to 0 for $He > 1$. Except for the weakest sources at low $He$, the statistic dispersion of values is also very marginal. In any of the three cases, OB and CLEAN-SC do not perform well for Helmholtz numbers below $He < 4$. However, as is shown later on, the deduction that those algorithms cannot be used for any case where $He < 4$ is of interest, is not correct. Interestingly, the OB algorithm seems to systematically underestimate the sound pressure levels, as the error median always is negative for the three cases. Moreover, the dispersion of error values is almost always higher than for the other sources, even for the strongest source at $He = 16$. DAMAS performs quite well, but slightly overestimates the levels of the strongest sources at higher $He$. For $He < 2$, it also tends to underestimate the level, albeit not to the extent of CLEAN-SC or OB. For the weakest source, DAMAS seems to become slightly unstable, as the dispersion of values even at high Helmholtz numbers is greater than for the other methods.

This is verified when plotting the level error against the difference between any source and the strongest source in its set, as is done for $He = 4$, $He = 8$, and $He = 16$ in figure 9. While CMF, OB, and CLEAN-SC show almost no dependency of the error on the level difference, the DAMAS results deviate more and more with higher level differences, underestimating the source levels of quieter sources. The high dispersion of error values for OB at $He = 4$ is in accordance with the generally poor performance of this algorithm at lower Helmholtz numbers as deducted from figure 8. The CMF algorithm again performs very well, with a very low error and dispersion.

The distance of the position of any source to the strongest source in the set, as is shown in figure 10, apparently does not have a very significant influence on the error levels for any of the algorithms. The slight increase of level median and dispersion visible at very low distances ($\Delta r < 0.1d$) can be attributed to (partial) inclusion of the stronger source in the circular integration sectors.

Figure 11 shows the level error of the sources depending on the distance to the nearest other source. The results look similar to what is shown in figure 10. However, here the level errors and dispersion from the OB calculations are lower even at $He = 4$, provided the distance to the nearest source is higher than ($\Delta r > 0.3d$). The higher the distance, the less the OB level error deviates from 0. The CLEAN-SC level error shows a similar, less pronounced characteristic.

With a level error criterion as is defined here, it is not possible to distinguish whether a method fails because the reconstructed level is actually to low or because the correct level is reconstructed at the wrong position. However, the objective is to accurately reconstruct both the level and the location of the sources, and for this, it delivers a single evaluation parameter for a vast parameter space.

Comparing the four methods with this error criterion, it was found that CMF delivers the best overall performance. DAMAS also delivers very good results. However, it tends to underestimate the levels of secondary sources. CLEAN-SC and especially OB have a higher error rate, in particular for lower frequencies.

Nevertheless, it has to be kept in mind that DAMAS and CMF are computationally rather costly and therefore cannot be applied under circumstances where calculation time is a critical issue (e.g. for 3D focus grids containing a large number of grid points[8]). If possible sources are not very close to each other and Helmholtz numbers above $He = 4$ are of interest, OB and CLEAN-SC will deliver a satisfying performance.

Furthermore, this study can only give a limited prediction whether these findings apply to actual measurements. It is not to be expected that OB or CLEAN-SC perform better than in the simulations, but the other algorithms may prove to be more sensitive to deviations from the assumed boundary conditions. Therefore, it is desirable for future work to expand the current boundaries, e.g. by incorporating into the simulations the directivity and correlation of sources, background noise or disturbances in the sound propagation.

However, each new addition to the complexity of the model results in a expansion of the possible parameter space, and the rules according to which the simulations are performed have to be chosen reasonably.

## IV. Conclusion

An approach to set up a testing system for the reliability of microphone array methods has been presented. It consists of defining boundary conditions corresponding to the intended use case and identifying parameters which may vary throughout the measurements. Reasonable assumptions on the nature of the parameter variations should be made and used as input for Monte Carlo simulations, which are used to generate data sets. These data sets are then processed with the microphone array methods of interest. It is desired for the methods to be able to determine the levels and locations of the sources correctly. The calculated results are therefore evaluated using a rating criterion suitable for these preconditions.

As exemplary case, a reliability study comparing four microphone array methods was performed. For the simulated scenarios, possible sources were constrained to be uncorrelated monopoles positioned in a plane parallel to the array. These scenarios had different number of sources, source positions and source levels. The rating criterion used was a sound pressure level error deduced from integrating reconstructed sound pressures over a fixed sector around the supposed source location. The results show that the proposed approach works and allows to evaluate microphone array methods depending on different parameters.

## V. Acknowledgement

This research was made possible by Deutsche Forschungsgemeinschaft under grant SA 1502/5–1.

## References

[1]Brooks, T. F. and Humphreys, W. M., "A deconvolution approach for the mapping of acoustic sources (DAMAS) determined from phased microphone arrays," *Journal of Sound and Vibration*, Vol. 294, No. 4-5, July 2006, pp. 856–879.

[2]Sijtsma, P., "CLEAN based on spatial source coherence," *International Journal of Aeroacoustics*, Vol. 6, No. 4, Dec. 2007, pp. 357–374.

[3]Sarradj, E., "A fast signal subspace approach for the determination of absolute levels from phased microphone array measurements," *Journal of Sound and Vibration*, Vol. 329, No. 9, April 2010, pp. 1553–1569.

[4]Yardibi, T., Li, J., Stoica, P., and Cattafesta, L. N., "Sparsity constrained deconvolution approaches for acoustic source mapping." *The Journal of the Acoustical Society of America*, Vol. 123, No. 5, May 2008, pp. 2631–2642.

[5]Yardibi, T., Zawodny, N. S., Bahr, C., and Liu, F., "Comparison of microphone array processing techniques for aeroacoustic measurements," *International Journal of Aeroacoustics*, Vol. 9, No. 6, 2010, pp. 733–762.

[6]Herold, G., Sarradj, E., and Geyer, T., "Covariance Matrix Fitting for Aeroacoustic Application," *AIA-DAGA 2013 Conference on Acoustics*, No. 11, Merano, 2013, pp. 1926–1928.

[7]Herold, G. and Sarradj, E., "Preliminary Benchmarking of Microphone Array Methods," *Proceedings of the 5th Berlin Beamforming Conference*, Berlin, 2014, pp. 1–13.

[8]Sarradj, E., "Three-Dimensional Acoustic Source Mapping with Different Beamforming Steering Vector Formulations," *Advances in Acoustics and Vibration*, Vol. 2012, 2012, pp. 1–12.

[9]Blacodon, D. and Elias, G., "Level Estimation of Extended Acoustic Sources Using a Parametric Method," *Journal of Aircraft*, Vol. 41, No. 6, Nov. 2004, pp. 1360–1369.

[10]Tibshirani, R., Johnstone, I., Hastie, T., and Efron, B., "Least angle regression," *The Annals of Statistics*, Vol. 32, No. 2, April 2004, pp. 407–499.

[11]Zou, H., Hastie, T., and Tibshirani, R., "On the "degrees of freedom" of the lasso," *Annals of Statistics*, Vol. 35, No. 5, 2007, pp. 2173–2192.

[12]"Acoular – Acoustic testing and source mapping software," *http://www.acoular.org*, 2015.

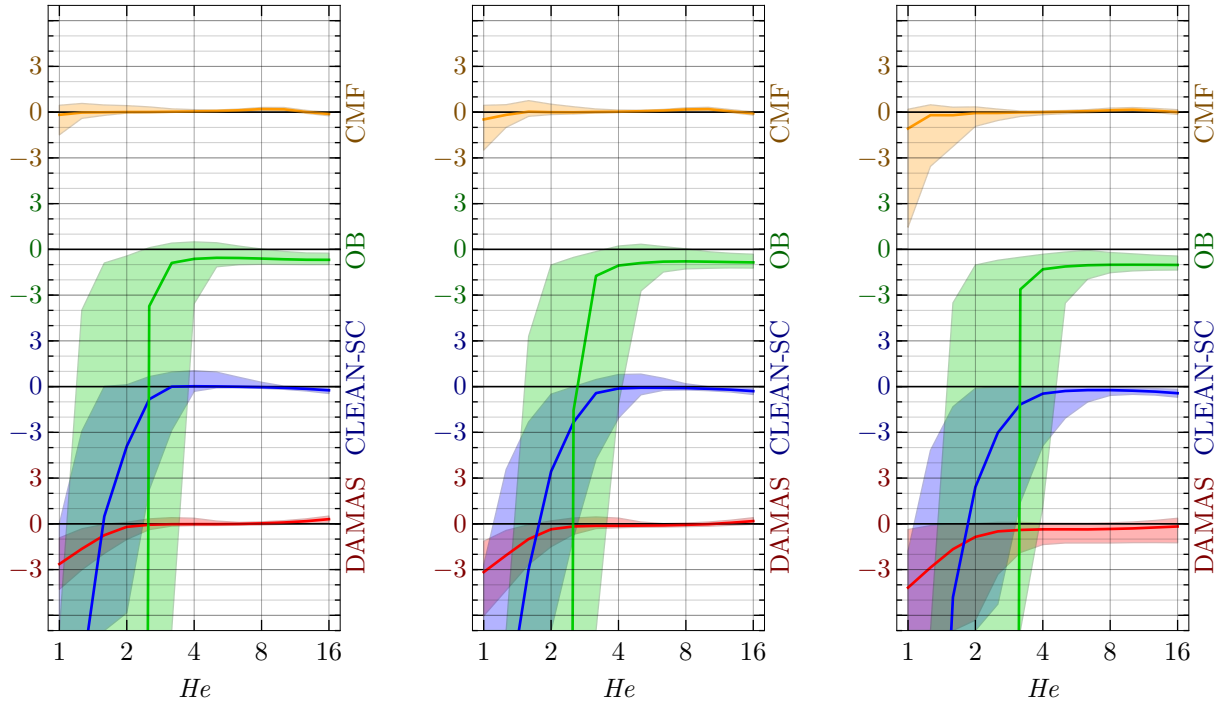


(a) Strongest source. (b) Second-strongest source. (c) Weakest source.

**Figure 8. Relative level error $\Delta L_{p,\mathrm{err}}$ in dB for different sources, depending on the Helmholtz number.**

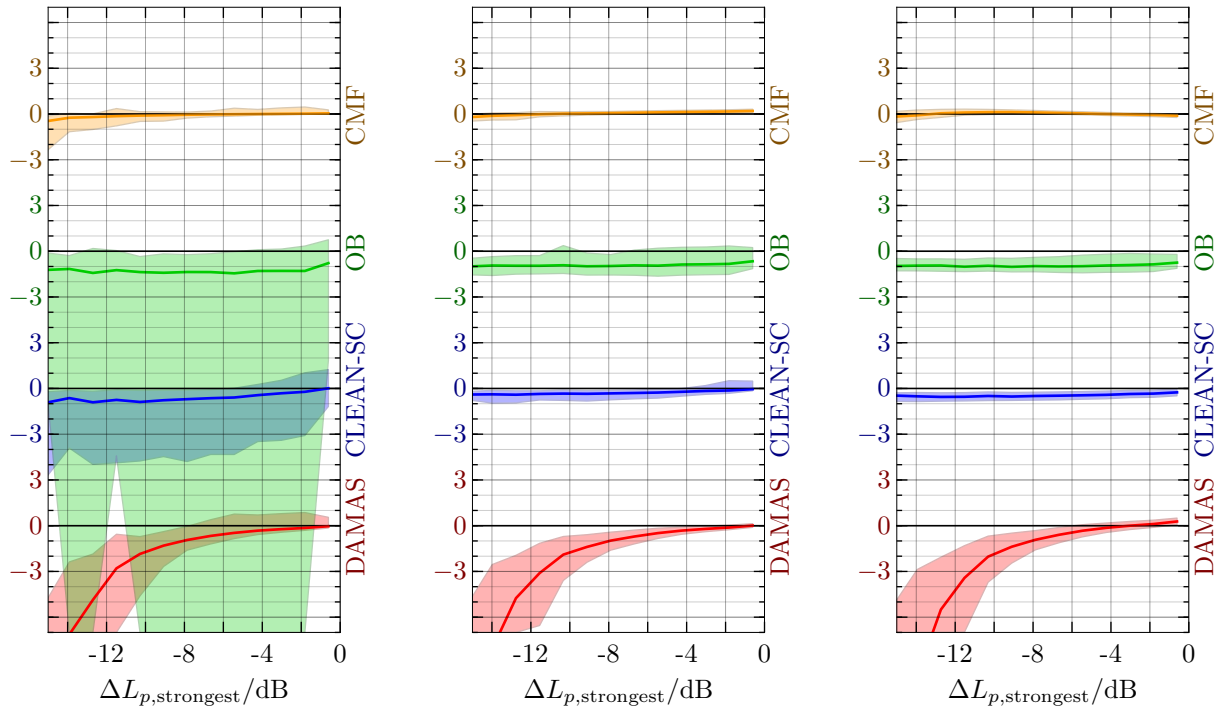


(a) $He = 4$. (b) $He = 8$. (c) $He = 16$.

**Figure 9. Relative level error $\Delta L_{p,\mathrm{err}}$ for different Helmholtz numbers, depending on level difference to the strongest source.**

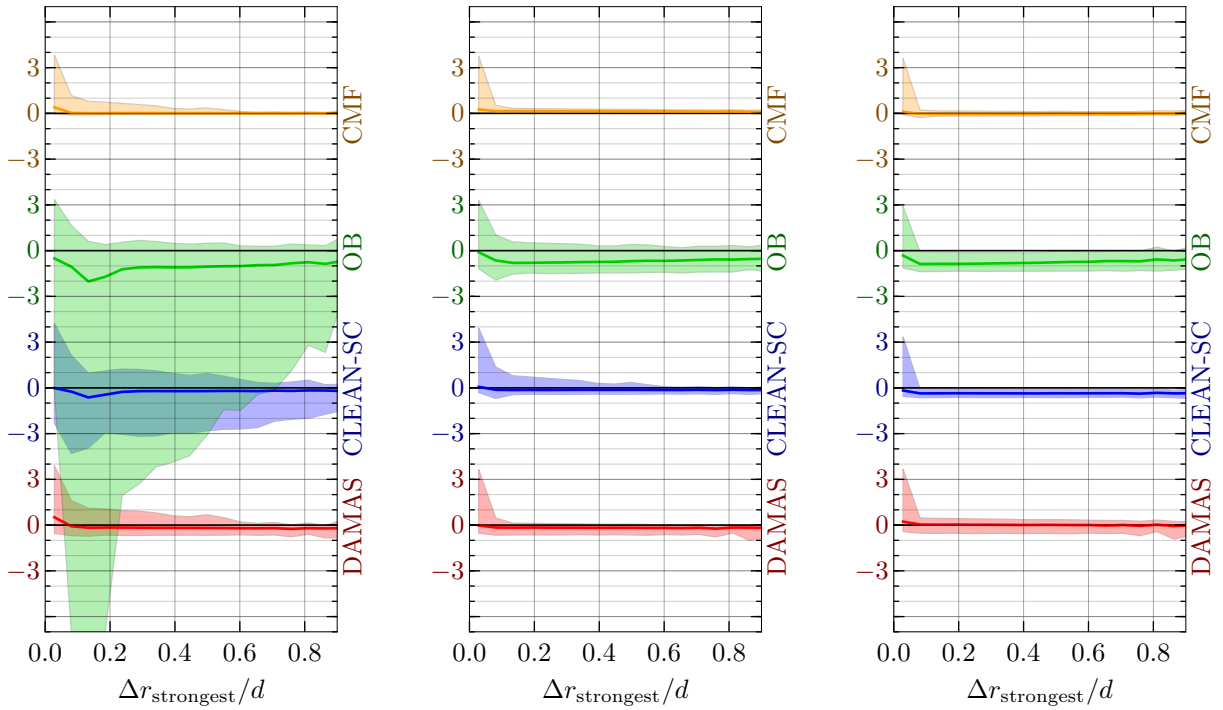


(a) $He = 4$. (b) $He = 8$. (c) $He = 16$.

**Figure 10. Relative level error $\Delta L_{p,\text{err}}$ for different Helmholtz numbers, depending on the distance of the evaluated source to the strongest source.**

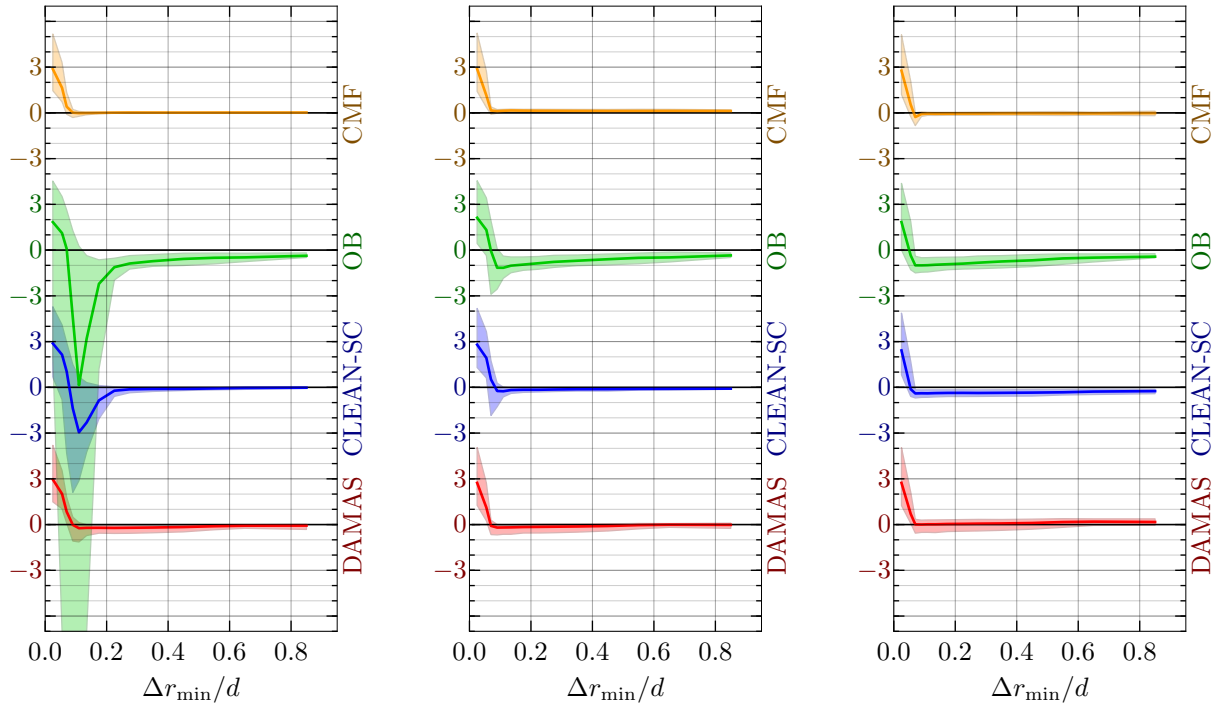


(a) $He = 4$. (b) $He = 8$. (c) $He = 16$.

**Figure 11. Relative level error $\Delta L_{p,\text{err}}$ for different Helmholtz numbers, depending on the distance of the evaluated source to the nearest source.**